

Location and Conformation of *n*-Alkanes in Zeolites: An Analysis of Configurational-Bias Monte Carlo Calculations

Simon P. Bates,^{*,†} Willy J. M. van Well, and Rutger A. van Santen

Schuit Institute of Catalysis, Laboratory for Inorganic Chemistry & Catalysis,
Eindhoven University of Technology, P.O. Box 513, 5600 MB Eindhoven, The Netherlands

Berend Smit

Shell International Oil Products, B.V. Shell Research and Technology Centre,
Amsterdam P.O. Box 38000, 1030 BN Amsterdam, The Netherlands

Received: May 14, 1996; In Final Form: August 13, 1996[⊗]

Results from calculations using a novel Monte Carlo method to simulate the sorption of *n*-butane to *n*-decane in various all-silica zeolites are analyzed to obtain information on the location and the conformation of the sorbed molecules. In general, the framework topology determines the conformation of the sorbed molecules. In mordenite, we find that butane is able to adsorb relatively unhindered, whereas longer chains are oriented parallel to the main channel direction and become less kinked with increasing carbon number. In ferrierite, butane molecules are distributed over both the 8- and 10-ring channels, while pentane and longer molecules are restricted to an all-*trans* conformation in the larger 10-ring channel. Faujasite appears to only slightly perturb the distribution of alkane conformations, compared to those found for gas phase alkanes. In zeolites rho and A, all alkanes are sorbed in a highly coiled conformation inside the α -cages of these structures.

1. Introduction

When considering interactions and reactions between zeolites and sorbed molecules, the location and conformation of guest molecules within the micropores can have a profound effect on the subsequent chemistry of these systems. Molecular level information on the location and conformation of sorbed molecules is not always readily accessible by experimental means, and recent advances in theoretical methods have made computer simulations an ideal candidate with which to address this problem.^{1–5} Energy minimization,¹ molecular mechanics,^{2–4} and Monte Carlo methods⁵ have all been used to study the location of *n*-alkanes in silicalite. In this paper we report an analysis of the location and conformation of *n*-alkanes from sorption calculations in a variety of all-silica zeolite lattices (MOR, FER, FAU, RHO, and LTA) carried out using a novel configurational-bias Monte Carlo method (CB-MC).

We have recently investigated the energetics of *n*-alkane sorption in a variety of all-silica zeolites, using the CB-MC technique.⁶ In that work, we had to examine the location and conformation of the sorbed molecules to fully understand the subtleties of the results and trends in the energy values. This is one particular example that illustrates the importance of a detailed description of where the adsorbed molecule is likely to be found within the zeolite and what kind of conformation it resides in. However, there are other, more general reasons that emphasize the importance of such information.

In the Results and Discussion section of this paper we show how certain regions of a particular zeolite's pore volume are inaccessible to some or all of the *n*-alkanes studied here. This confinement to certain regions of the pore and not others can have far-reaching implications for the catalytic behavior of such a system. Reactants may be excluded from approaching acid sites that are located within these inaccessible pore regions. In

addition to the preferred location of the molecule within the zeolite, the conformation it adopts is dependent (amongst other things) upon the topology of the pore system and the length of the alkane. In the Results and Discussion section, we give examples of zeolites that confine alkane chains in highly coiled conformations and others that enforce all-*trans* conformations. These two extreme cases produce different entropy changes on sorption, and it is quite possible that sorbates of different conformation may behave differently toward a particular reaction.

The following sections of this article contain a brief description of the analysis method, a section of results and discussion, and finally the conclusions that may be drawn from this study.

2. Calculation Details

The results described in this paper are derived from data collected during a series of configurational-bias Monte Carlo (CB-MC) calculations simulating the sorption of alkanes butane to decane in a variety of all-silica zeolites. The CB-MC technique is a novel Monte Carlo method for the simulation of chain molecules, the details of which have been extensively described in previous publications^{5,7} and will not be reiterated here. The procedure "grows" alkane chains atom by atom inside the zeolites. This avoids a major disadvantage that is inherent in conventional Monte Carlo methods, *i.e.* the rapid decrease in probability of accepting a trial insertion as chain length increases. In this work, we have assumed a fixed zeolite lattice, according to the work of Kiselev *et al.*⁸ Thus, the polarizability of the lattice is ignored, and we assume that the location and conformation are principally governed by the fit of the molecule inside the pores. While it is clear that framework distortions can markedly affect the migration of adsorbates through the micropores,⁴ the "static" simulations using the CB-MC method are likely to be far less dependent on the flexibility or rigidity of the framework. The simulations have all been performed at infinite dilution, *i.e.* one alkane molecule inside the zeolite host, at a temperature of 298 K. It has been noted that different loadings alter the conformations of sorbed species far less than

* Corresponding author.

[†] Present address: Department of Physics, Keele University, Keele, Staffs ST5 5BG, UK.

[⊗] Abstract published in *Advance ACS Abstracts*, October 1, 1996.

other variables, such as simulation temperature.⁴ The source of framework atom coordinates for the zeolite models used in the calculations is detailed in the Appendix, along with the intermolecular potential parameters employed.

In this section, we give a description of the sampling procedure used to investigate the distribution of the alkanes within the zeolites and subsequent conformational analysis. At regular intervals during the simulations (usually every 5000 cycles) a snapshot of the sorbed alkane is stored. After a sufficient number of snapshots have been taken (approximately 10 000), the end-to-end vector of each conformation is determined and also the projection of this vector on each of the x -, y - and z -axes. If the normalized component of the end-to-end vector projected along the x -axis is greater than a certain value (R), this particular alkane is deemed to be parallel to the x -axis. If the normalized component projected onto the y -axis is greater than R , the alkane is parallel to the y -axis and so on for the z -component. In these calculations we have used an R value of 0.707. The exact distribution is dependent on the precise value of R that is used, though not critically. As a result of this, our discussions focus on the qualitative trends illuminated by this analysis, rather than exact values. It is noted here that throughout the paper we abbreviate “oriented in such a way that the normalized component of the end-to-end vector projected onto the x -axis is greater than R' to “oriented parallel to the x -axis”.

This division of the conformations by orientation of the end-to-end vector of the alkane provides information as to the distribution of the alkanes over the channels in the zeolite; for all the zeolites we studied except FAU, the channel directions are parallel to one or more of the crystallographic axes. In the case of highly symmetric cubic zeolites such as RHO or LTA, there is no difference between the x -, y -, and z -directions. However, in other cases, such as MOR and FER, this division into x -, y -, and z -directions proves to be invaluable in probing the location of the sorbed species.

The conformations of the molecules parallel to each of the three crystallographic axes are analyzed individually. By doing this, we can show conformational differences for alkanes sorbed in different zeolite channels or different orientations within the same channel. In addition, we can obtain information on the effect of confinement in the zeolite channel on the conformation of the alkane. This is done by comparing the conformation of alkanes within a zeolite to those from simulations performed without a zeolite lattice present. Differences between the free, or “gas phase”, data and those for molecules within the zeolite can then be attributed to location and/or conformation within the pores. We have analyzed the conformations on a per bond and a per chain basis; that is, the results are presented as total distribution of dihedral angles over all bonds and number of gauche bonds per chain. We also analyze the probability of finding a gauche bond as a function of position in the carbon backbone. This kind of conformational analysis has been applied to alkanes sorbed in silicalite in a previous publication.⁵

3. Results and Discussion

(a) Mordenite. Mordenite is widely used as a solid-acid catalyst and has a pore structure that is effectively unidimensional. An elliptical 12-ring channel ($7.0 \text{ \AA} \times 6.5 \text{ \AA}$) runs parallel to [001] and has small side pockets parallel to the [010] direction. This suggests that the distribution of the alkane end-to-end vectors is likely to be exclusively parallel to the [001] crystallographic axis. However, analysis predicts that for butane a significant proportion (approximately 20%) of alkane chains have an end-to-end vector parallel to the x -axis (the direction

of the 7.0 \AA pore diameter). A small proportion (approximately 5%) align parallel to the y -axis, the direction of the 6.5 \AA pore opening, and the remainder are parallel to the z -axis. The small proportion of butane molecules that are found parallel to the y -axis would suggest that the side pockets are effectively inaccessible. This has also been observed experimentally in a recent study of alkane sorption in H-MOR.⁹ The butane molecule appears to be relatively unconstrained inside the pores of mordenite; it sorbs in a variety of different orientations.

When the chain length increases by just one carbon atom, the lack of constraint exhibited by the butane molecule disappears. In the case of pentane, over 95% of all alkane chains align parallel to the z -axis. The remainder that are perpendicular to the main pore direction are the molecules with highest energy in the simulations, irrespective of their conformation. Increasing the chain length to six or more carbon atoms results in molecules that adsorb with end-to-end vectors exclusively parallel to the z -axis.

When analyzing the conformations of the sorbed alkanes in mordenite, it is important that we have information on the conformations of the free alkanes, without any zeolite present. A conformational analysis of the free “gas phase” alkanes butane to decane is presented in Figure 1a,b,c. The upper graph shows the distribution of dihedral angles over all bonds in each of the alkanes. The middle graph shows the relative proportions of chains with a given conformation (all-*trans*, one gauche bond, etc.), and the bottom graph shows the probability of finding a gauche bond at a certain position along the alkane backbone.

A number of features are worth highlighting on these graphs. Firstly, the total proportion of *trans* bonds is the same for all the alkanes studied here (approximately 70%). Also, the most commonly occurring conformation for the chains is all-*trans* for butane, all-*trans* or one gauche bond for pentane, one gauche bond for hexane and heptane, one or two for octane, and two for nonane and decane. Finally, the probability of finding these gauche bonds at a certain point in the chain is largest for the terminal bonds for all alkanes studied (though octane, nonane, and decane do have a relatively high probability of having a gauche bond near the midpoint of the backbone). The conformations represented in Figure 1 are in good agreement with literature data determined from experimental studies.^{10,11} The first of these¹⁰ reports 32% of *n*-butane molecules in the gas phase are found to contain a gauche bond at 298 K, a figure calculated from the Raman spectrum. The equivalent value from our simulations is 33%. The second¹¹ gives proportions of different conformations calculated from an electron diffraction study of gaseous *n*-alkanes. Percentages of all-*trans* conformations of gaseous *n*-pentane, *n*-hexane, and *n*-heptane are 38%, 25%, and 16%, respectively. Our simulations predict values of 45%, 30%, and 19%.

Figure 2 shows an equivalent conformational analysis for alkanes sorbed in the pores of mordenite. In Figure 2a,b, a distinction is made between the butane molecules that adsorb parallel to the main channel [001] and those that adsorb parallel to the x -axis. Those molecules that adsorb parallel to the x -axis have a far higher total proportion of gauche bonds and a greater number of chains containing a gauche bond than those parallel to the z -axis. This is in accordance with the pore structure of mordenite; the constraint of the zeolite lattice forces most butane molecules parallel to the x -axis to adopt a twisted structure.

For those butane molecules that are parallel to the z -axis, and for pentane and higher alkanes, the total percentage of *trans* bonds increases with chain length. This is in contrast to the behavior of the free alkanes, detailed above. We also observe a different distribution of the number of gauche bonds in a chain;

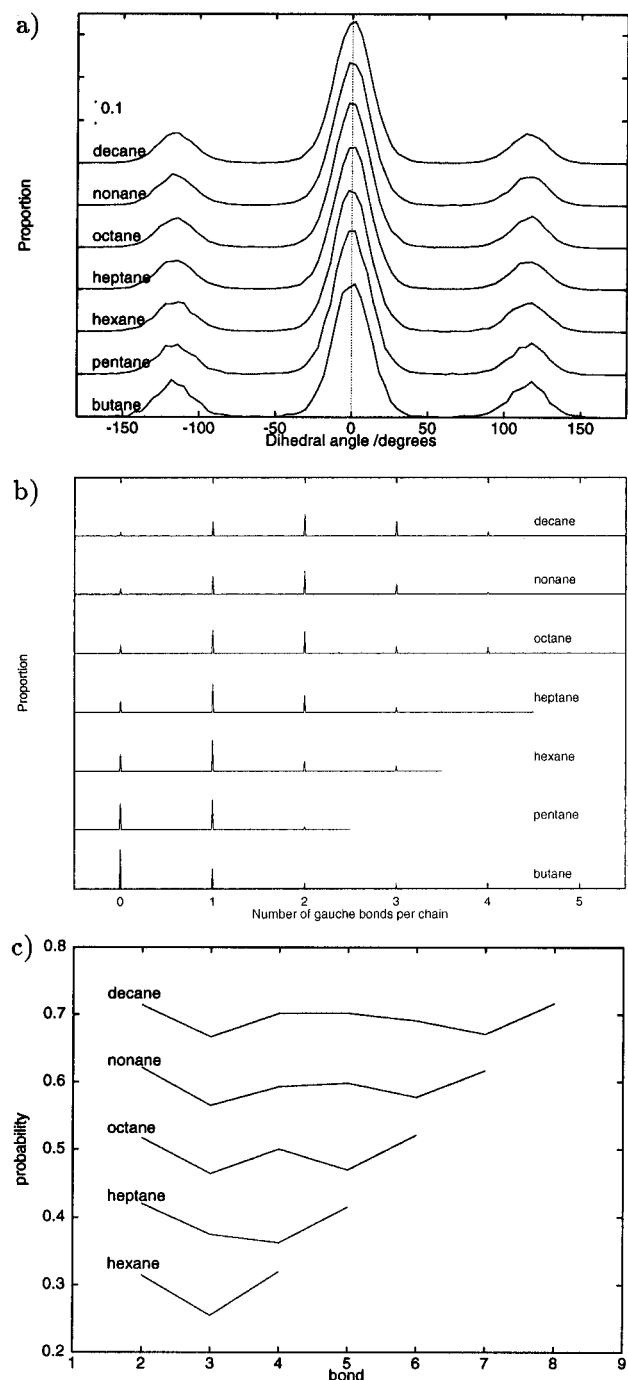


Figure 1. Conformational analysis of free alkanes. (a) Total proportion of bonds as a function of dihedral angle (0° corresponds to a *trans* conformation; the scale bar indicates the proportion). (b) Number of gauche bonds per alkane chain. (c) Probability of finding a gauche bond as a function of position in the chain (the curve of heptane is shifted by +0.1, octane by +0.2, etc.).

the minimum percentage of alkanes in mordenite that are either in the all-*trans* conformation or have only one gauche defect is 60%. In the case of the free alkanes, this value is only 30%. Thus, alkanes in the [001] channel of mordenite tend to be straighter than their free counterparts, due to the presence of the zeolite lattice. The alkanes are not forced to be totally straight: the pore diameter of mordenite is substantially larger than the cross-sectional diameter of an *n*-alkane and the chains parallel to the *z*-axis need not be in the all-*trans* conformation. More than 10% of decane molecules have three gauche defects; although this is less than half the value for free decane, it is nonetheless significant.

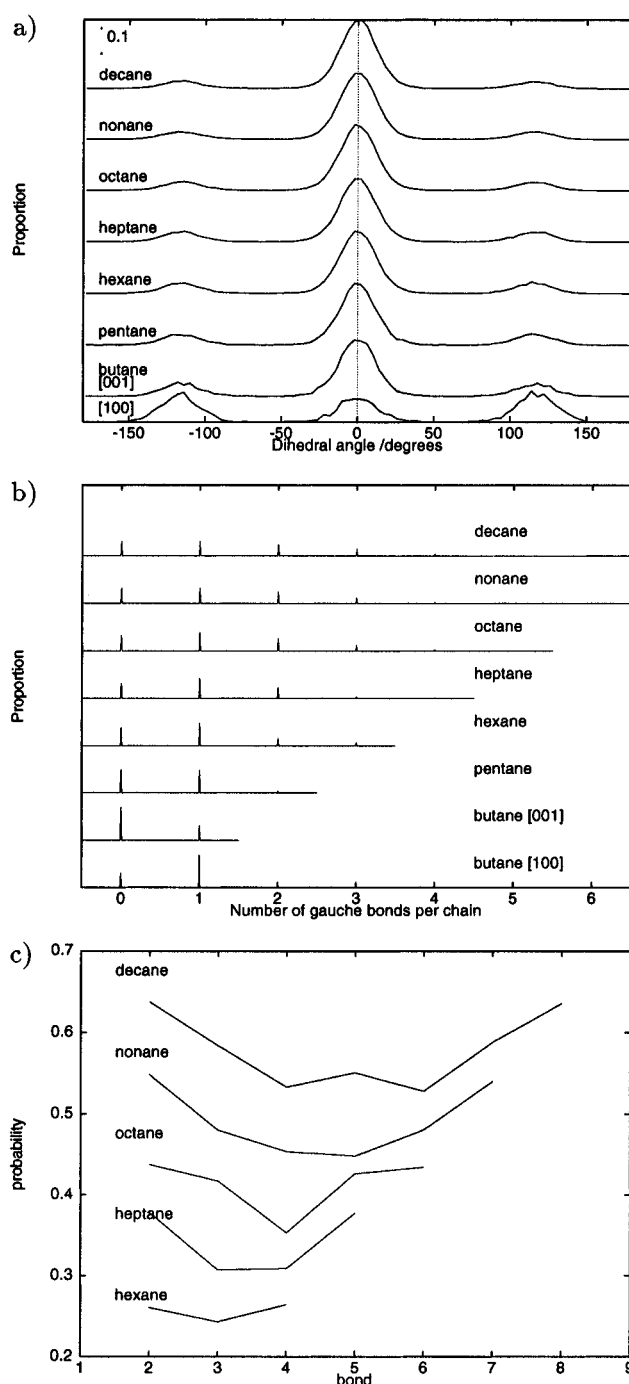


Figure 2. Conformational analysis of alkanes in mordenite. (a) Total proportion of bonds as a function of dihedral angle (0° corresponds to a *trans* conformation; the scale bar indicates the proportion). (b) Number of gauche bonds per alkane chain. (c) Probability of finding a gauche bond as a function of position in the chain (the curve of heptane is shifted by +0.1, octane by +0.2, etc.).

The probability distribution of finding a gauche bond at a certain position in the chain of hexane and higher alkanes is similar to the case for the free alkanes. Sorption inside mordenite seems to strengthen the trend that a gauche bond is most likely to be found at either end of a chain.

In summary, sorption of butane in mordenite appears to be relatively unconstrained, though those molecules that lie perpendicular to the main pore are more kinked. Pentane and higher alkanes align exclusively with the direction of the main channel, [001]. Those molecules that lie parallel to [001] are generally less kinked compared with free alkanes, and this trend increases with chain length.

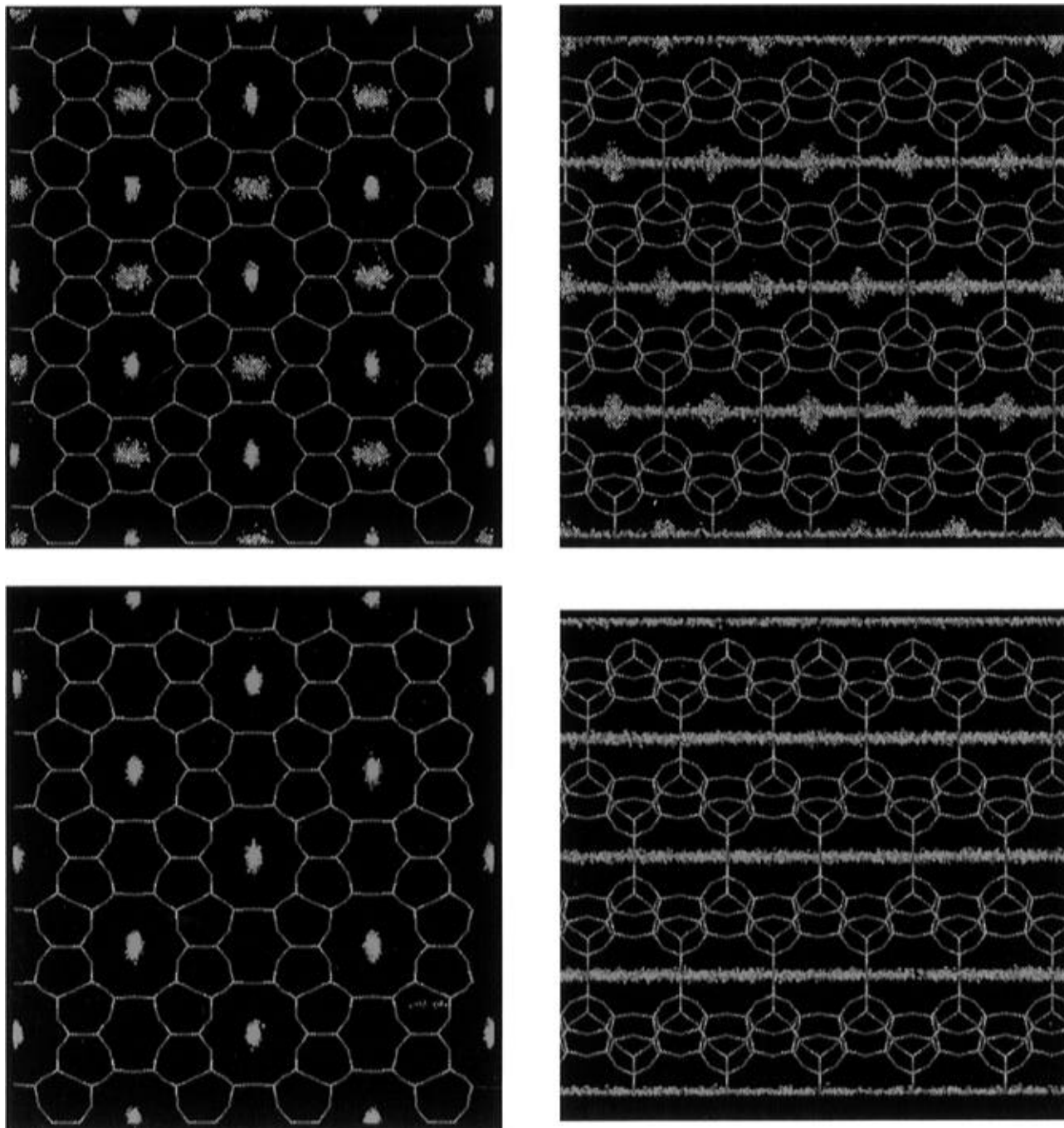


Figure 3. Distribution of *n*-butane (upper two figures) and *n*-decane (lower two figures) in ferrierite. (Each dot represents the middle of the carbon backbone; the molecules aligned parallel to the *y*-axis are colored gray; those parallel to the *z*-axis are blue; the left-hand figures are viewed down [001], the right-hand down [010].)

(b) Ferrierite. Ferrierite is a zeolite that contains two intersecting straight channels: a 10-ring ($5.4 \times 4.2 \text{ \AA}$) parallel to [001] and an 8-ring ($4.8 \times 3.5 \text{ \AA}$) parallel to [010]. Its application as a commercial solid-acid catalyst has been restricted by stacking faults in the material, but it has nonetheless been shown to be an excellent shape-selective isomerization catalyst for the production of isobutene, feedstock for the production of methyl *tert*-butyl ether (MTBE).¹² It is particularly interesting as it yields large heats of adsorption for straight chain alkanes, as we have discussed in a previous publication.⁶

For the sorption of butane in ferrierite, approximately one-third of the butane molecules are found to be parallel to the [010] direction, which is the direction of the smaller 8-ring channel. The remaining butane molecules adsorb parallel to the [001] direction, the direction of the larger 10-ring channel.

For pentane and higher alkanes, all molecules are located parallel to [001]. Thus, ferrierite appears to be a zeolite that is two-dimensional to butane (and presumably shorter alkanes) and unidimensional to pentane and higher alkanes. Such a boundary between two- and one-dimensional behavior is likely to be sensitive to, for example, different partial pressures of adsorbate and different temperatures.

Figure 3 shows the distribution of *n*-butane and *n*-decane within the ferrierite pore system. The upper two pictures show the locations of the center of the carbon backbone of 10 000 butane molecules; the lower two pictures show decane. The pictures on the left of the figure are viewed down [001], while those on the right are viewed down [010]. The figure clearly shows that *n*-butane molecules are distributed over the two channels, while the *n*-decane molecules are confined to the larger

10-ring channel. The butane molecules that adsorb parallel to the *y*-axis (gray dots) are localized in the center of the 8-ring channels, while those parallel to the *z*-axis (blue dots) are distributed evenly throughout the 10-ring channel.

The cross-sectional diameter used in this study for the *n*-alkane molecules (3.9 Å) is very close to the average pore diameter of the 8-ring channel of ferrierite (4.1 Å). It is worth considering the possibility of migration of a butane molecule from the larger 10-ring channel into the smaller channel via an 8-ring window. The barrier to diffusion through such an opening may be expected to be high, but may be reduced by the flexing of the framework. An MD study of methane diffusion in dealuminated zeolite A has been reported by Demontis and Suffriti.¹³ They demonstrate that diffusion of the methane through the 8-ring windows that allow access into the α -cages is controlled by the breathing of these windows; calculated diffusion coefficients are 1 order of magnitude lower if the framework is kept rigid during the simulations. The barriers to diffusion through the 8-ring in ferrierite may be similarly affected by framework distortions.

In Figure 4 we present an analysis of the dihedral angles of the alkanes sorbed in ferrierite; Figure 4a shows the total dihedral distribution on a per bond basis, and Figure 4b on a per chain basis. Figure 4c shows the probability of finding a gauche bond at a certain point in the alkane chain. These graphs illustrate the confinement of the molecules within the channels. For the butane molecules in [010], Figure 4a,b shows that they are far more coiled than their gas phase counterparts (Figure 1a,b). For those alkanes confined to the larger 10-ring channel, the general trend is toward all-*trans* molecules. Thus, in contrast to the case for longer chain alkanes in mordenite described earlier, sorption in the 10-ring of ferrierite forces the molecules to adopt a completely straight conformation. The probability of finding a gauche bond at a certain point in the chain is approximately constant and far lower compared to the cases of either the gas phase alkanes or those adsorbed in mordenite. This is reflected in the scale on the *y*-axis of Figure 4c.

In summary, the sorption of alkanes in ferrierite produces a number of interesting features. Butane molecules are distributed over both the smaller and the larger channel in an approximate ratio of 1:2. For pentane and larger molecules, sorption is exclusively in the 10-ring channel and the vast majority of these molecules are in the all-*trans* conformation.

(c) Faujasite. Faujasite is a cubic zeolite, with 12-ring openings of 7.4 Å parallel to [111] that provide access to a supercage of diameter 12.5 Å. In such a case, there is no need to segregate the alkanes into those parallel to the three crystallographic axes. Of the all-silica zeolites considered in this work, faujasite has the largest pore dimensions, and this, together with its widespread use in industrial processes, principally as an fcc catalyst, makes it of particular interest.

Our analysis of the distribution of the alkanes in faujasite shows that all parts of the pore system are visited by all alkanes (butane to decane) during the course of the simulations. This is to be expected, as the large pore diameters are unlikely to exclude molecules in the same way we have seen for ferrierite, and is a good indicator of the reliability of the CB-MC calculations.⁵ In Figure 5 we present an analysis of the conformation of the sorbed alkanes.

An immediate correspondence can be seen between the conformations of the alkanes adsorbed in faujasite and those of the free, gas phase molecules (Figure 1). The same trends can be observed in the curves on Figure 5 and Figure 1, and the actual data values are also similar; for example, in faujasite the total percentage of *trans* bonds present in the sorbed alkanes

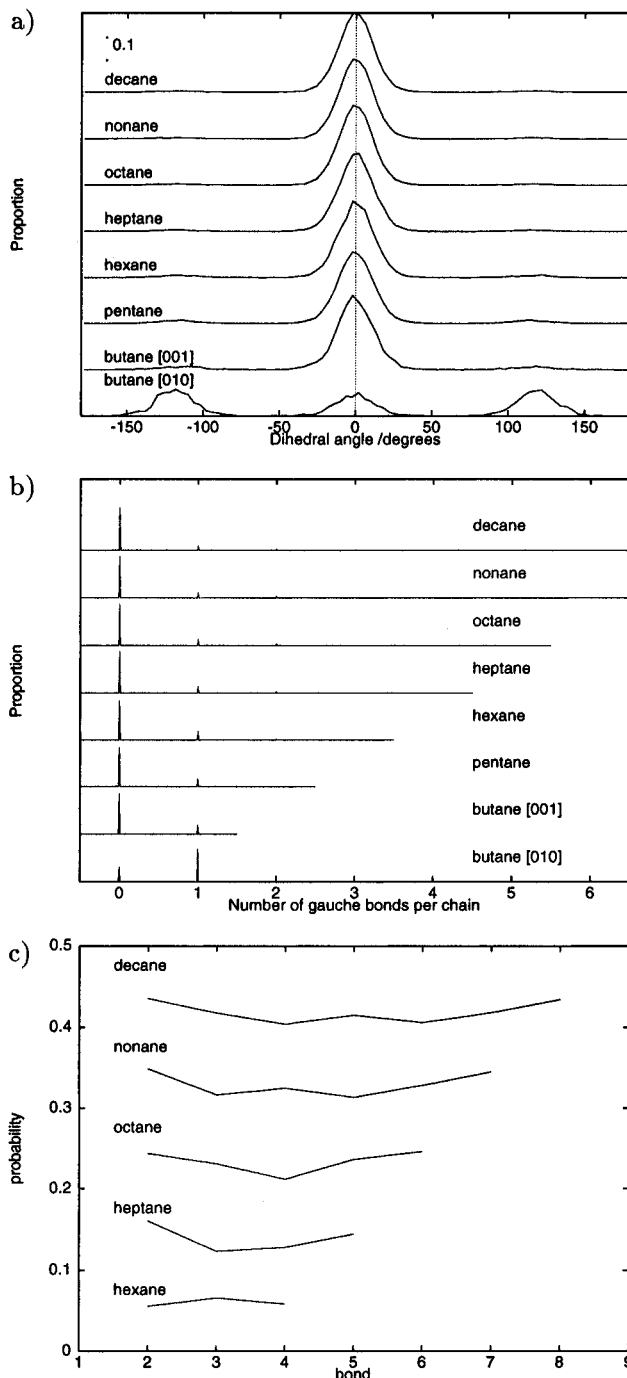


Figure 4. Conformational analysis of alkanes in ferrierite. (a) Total proportion of bonds as a function of dihedral angle (0° corresponds to a *trans* conformation; the scale bar indicates the proportion). (b) Number of gauche bonds per alkane chain. (c) Probability of finding a gauche bond as a function of position in the chain (the curve of heptane is shifted by +0.1, octane by +0.2, etc.).

stays approximately constant as the chain length increases. The profiles of the number of gauche bonds per chain are similar for the free alkanes and those adsorbed in the pores of faujasite, as are the probabilities of finding a gauche bond at a certain point in the chain.

We may conclude from this analysis that faujasite is a zeolite whose pore system places little or no constraint on the location and the distribution of the alkanes sorbed within it at low concentration, so close is the agreement between the conformations of the sorbed and gas phase molecules. This is in agreement with what we would intuitively expect from this zeolite, given a knowledge of its pore dimensions.

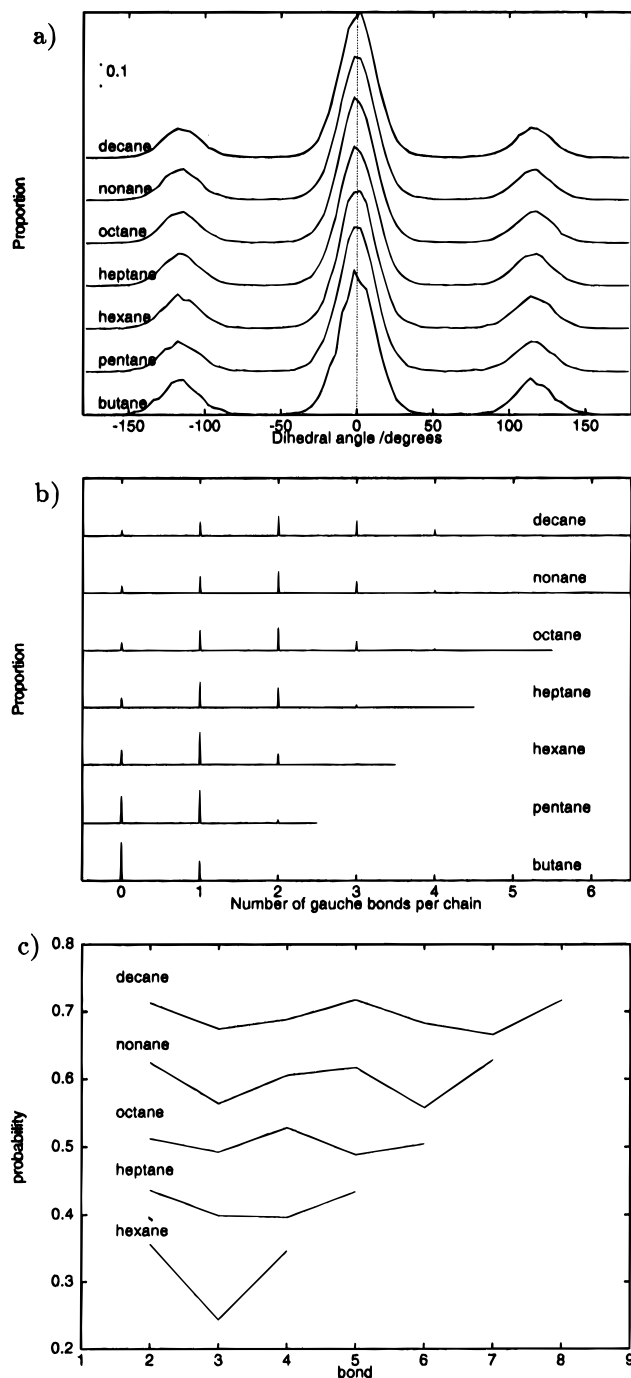


Figure 5. Conformational analysis of alkanes in faujasite. (a) Total proportion of bonds as a function of dihedral angle (0° corresponds to a *trans* conformation; the scale bar indicates the proportion). (b) Number of gauche bonds per alkane chain. (c) Probability of finding a gauche bond as a function of position in the chain (the curve of heptane is shifted by +0.1, octane by +0.2, etc.).

(d) Zeolite rho. Zeolite rho possesses the smallest pore openings of the zeolites described in this study: 3.6 Å. It is a cubic material composed of α -cages linked via double-8-rings. It has been reported as a particularly efficient catalyst for the reaction of methanol and ammonia to selectively produce dimethylamine.¹⁴

We have briefly discussed the location of alkanes in zeolite rho in a previous publication concerned with the energetics of *n*-alkane sorption in all-silica zeolites.⁶ We find that irrespective of chain length, the sorbed alkanes studied in this work are all found in the center of the α -cages of RHO, the largest available void volume. This is in stark contrast to the situation for

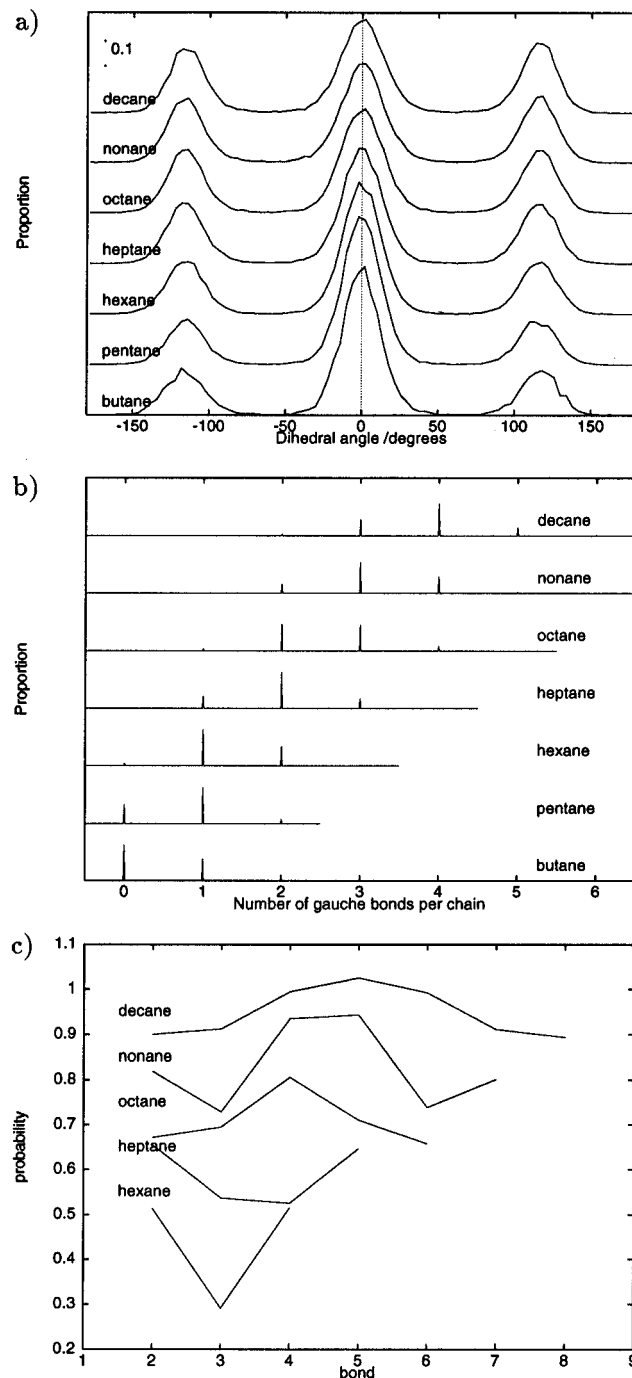


Figure 6. Conformational analysis of alkanes in zeolite rho. (a) Total proportion of bonds as a function of dihedral angle (0° corresponds to a *trans* conformation; the scale bar indicates the proportion). (b) Number of gauche bonds per alkane chain. (c) Probability of finding a gauche bond as a function of position in the chain (the curve of heptane is shifted by +0.1, octane by +0.2, etc.).

faujasite, described above, where all parts of the pore system are accessible. This location for sorption seems always to be more favorable than locating any of the alkane molecules in the double-8-rings that connect the cages. We have previously noted that even in the case of decane adsorbed in rho, the whole of the carbon backbone is found to be within the α -cage; not even the end CH_3 groups extend into the double-8-rings. This highly localized confinement in a relatively small void space has a dramatic effect on the conformation of the sorbed alkanes.

Figure 6 shows conformational analysis graphs for butane to decane in zeolite rho. If a *similarity* was obvious between the alkanes in faujasite and those in the gas phase, a *difference*

between the gas phase alkanes and those in rho is just as apparent. The confinement within the α -cages leads to alkane chains that are highly coiled. Figure 6a reflects this in a high proportion of gauche bonds, compared with the gas phase case shown in Figure 1a. The total percentage of gauche bonds for alkanes sorbed in rho increases with increasing carbon number; approximate values are 40% for butane and 60% for decane.

The number and distribution of gauche bonds in each chain is very different from the free alkane case, as a comparison of Figures 6b and 1b shows. In zeolite rho, pentane is the largest alkane for which any all-*trans* conformations are found. This is to be compared to the free alkane case, in which approximately 10% of all octane and nonane molecules are found to possess an all-*trans* conformation. The average number of gauche bonds per chain for the curves in Figure 6b shows a gradual increase with increasing carbon number. This is in accordance with the location of the sorbed alkanes; longer chains occupying the same void volume must become progressively more coiled. The probability of finding a gauche bond at a certain position in the carbon chain for octane and longer alkanes shows a reverse trend compared with the free, gas phase data. In this case it appears more likely that a gauche bond is found at or near the middle of the chain. It is also clear from the *y*-axis scale in Figure 6c that the probability of finding a gauche bond *anywhere* in the chain is higher than the free alkane case.

It is interesting to investigate if this coiling is seen in alkanes of far higher molecular weight than decane. We have performed supplementary calculations on the sorption of eicosane ($C_{20}H_{42}$) in zeolite rho. The results show that the sorbed alkane is still completely contained within the α -cage, though in a very twisted conformation; 90% of all chains include nine or more gauche defects. By contrast in the gas phase, the average number of gauche bonds per eicosane chain is 5 or 6. The heat of adsorption of eicosane in zeolite RHO is estimated to be 140 ± 5 kJ/mol. We have previously found⁶ that the heat of adsorption of *n*-butane to *n*-decane in RHO obeys the equation $Q = 6.3n + 5$ kJ/mol, where *n* is the carbon number, which predicts a heat of adsorption of 131 kJ/mol for eicosane, assuming linear behavior extends as far as C_{20} . These two values show reasonable agreement. Sorption is predicted to be thermodynamically favorable for chains as long as C_{20} , in agreement with a similar CB-MC study into the sorption of alkanes in silicalite.^{15,16}

As the chain length is increased still further, the sorption of the alkane contained completely within a single α -cage may become energetically unfavorable and/or the two ends of the alkane will be located in neighbouring α -cages, with a section of the middle of the chain passing through the energetically unfavorable region of the double-8-ring windows. We are presently performing calculations to investigate this using octatetracontane ($C_{48}H_{98}$).

In summary, the sorption of alkanes in zeolite rho is confined exclusively to the α -cages and results in drastic conformational changes compared to the free, gas phase alkanes. The highly coiled sorbed alkanes possess a relatively high intramolecular potential compared to the free alkanes, and it is very likely that this will have an effect on the properties and subsequent reactivity of such species. This highly coiled behavior in zeolite RHO extends to at least C_{20} .

(e) Zeolite A. Zeolite A has a similar framework structure to that of rho; in zeolite A the α -cages are connected via single-8-rings. Whereas the body-center of the RHO unit cell contains an α -cage, the center of the LTA cell contains a β -cage. Zeolite A has pore openings that are approximately 0.5 Å larger than those of RHO (4.1 Å). The reason for this is that the

as-synthesized crystal structure we used to construct the zeolite contains a significant amount of aluminum. (It should be stressed once again here that the as-synthesized crystal structure was used only to build the zeolite lattice; during the simulations all T atoms were set to silicon.)

A large proportion (over 50%) of the butane molecules are inserted and grown inside this central β -cage during the simulations. Experimentally, or in a MD study, it is highly unlikely that butane molecules can migrate through the 6-ring windows of the β -cage. To make the calculations of sorption of butane more realistic, we blocked off the β -cages by inserting a single oxygen atom into the center of each cage. This yields a energy value (29.0 kJ/mol) that is close to what we would expect on the basis of the incremental heat of adsorption per C atom determined for C_5 to C_{10} . Moreover, the heats of adsorption of longer alkanes (that do not insert and grow inside the β -cages) are found to be hardly altered by this correction.⁶

Once this correction has been applied, we can investigate the conformations of the sorbed molecules. As in the case of RHO, the alkanes are found inside the α -cages in a coiled conformation. Figure 7 shows the conformational analysis for alkanes sorbed within zeolite A. The general features and trends in the curves are similar to those seen for sorption in zeolite rho (Figure 6), though deviations from the gas phase behavior are less extreme as the void volume of the α -cages are slightly larger. One example of the similar trends between alkanes in zeolites A and rho is the increase in total percentage of gauche bonds with increasing carbon number, as shown in Figure 7a. This increase is far less marked for zeolite A than for rho. In Figure 7b, the graphs of number of gauche bonds per chain show a greater proportion of less coiled chains compared to rho.

In summary, the location of alkanes sorbed in zeolite A is similar to those in zeolite rho: the α -cages. A computational difficulty (butane growing inside the β -cages) is resolved by blocking these pores with a single oxygen atom. The conformations of the alkanes in zeolite A are less tortuous as a result of the slightly larger cage volume in this material.

4. Conclusions

The analysis of a series of CB-MC simulations has generated a great deal of information on the location and conformation of *n*-alkanes sorbed in a series of all-silica zeolites. The conclusions for each zeolite studied are briefly stated below.

(i) In mordenite, butane adsorbs relatively unconstrained by the zeolite lattice. A significant proportion of butane molecules align perpendicular to the channel down [001]. For longer alkanes the pore geometry forces the alkanes parallel to the [001] direction and the sorbed molecules become less kinked with increasing carbon number.

(ii) In ferrierite, butane is distributed over the 8- and 10-rings in a ratio of approximately 1:2. Pentane and higher alkanes are found to reside only in the larger channel in an all-*trans* conformation. Therefore, at the conditions imposed by our calculations (infinite dilution and a temperature of 298 K), certain regions of the ferrierite pore structure appear to be inaccessible to pentane and longer alkanes. This distribution may also be a function of the flexibility or rigidity of the framework.

(iii) Sorption in the large supercages of faujasite results in alkane conformations that are very similar to those found in the gas phase. In other words, the alkane molecules are stabilized by the zeolite, but the pore dimensions are large enough for this stabilization not to force large conformational changes in the sorbed alkanes.

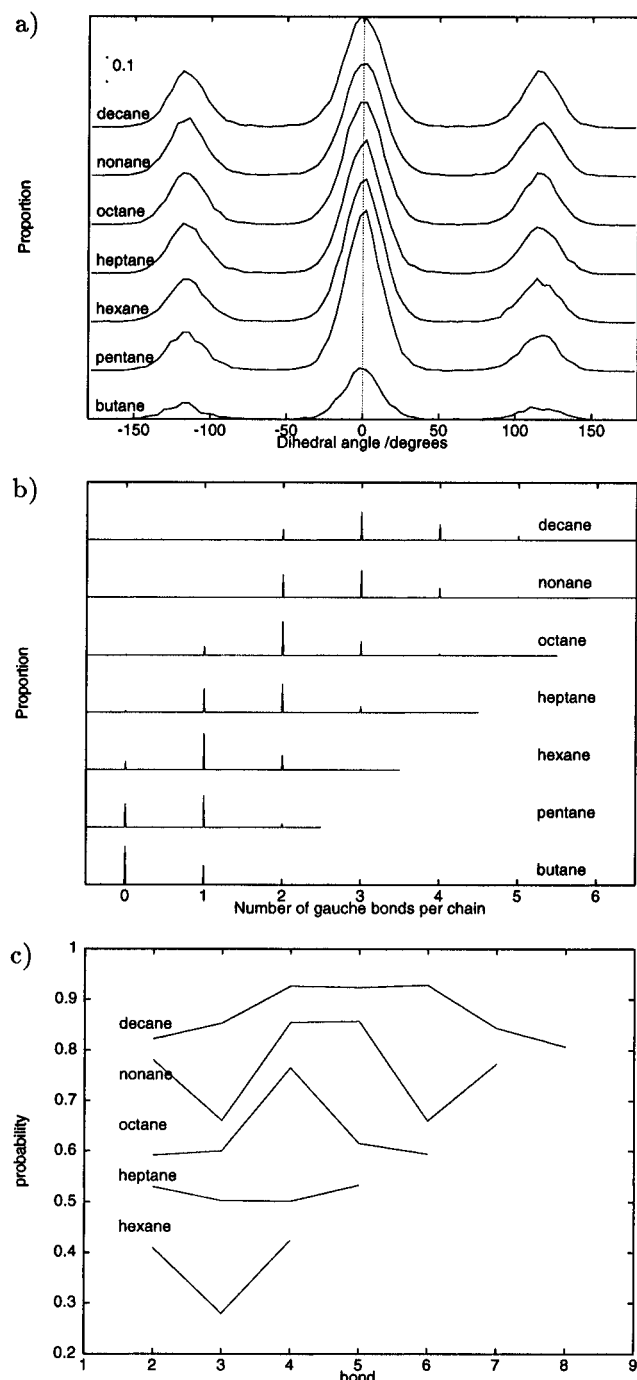


Figure 7. Conformational analysis of alkanes in zeolite A. (a) Total proportion of bonds as a function of dihedral angle (0° corresponds to a *trans* conformation; the scale bar indicates the proportion). (b) Number of gauche bonds per alkane chain. (c) Probability of finding a gauche bond as a function of position in the chain (the curve of heptane is shifted by +0.1, octane by +0.2, etc.).

(iv) In the small-pore zeolites rho and A, the alkanes are found to adsorb exclusively in the α -cages of the structure in a highly coiled conformation. The effect is most dramatic in zeolite rho, in agreement with the smaller pore diameter.

The precise distribution and conformation of the alkane molecules in the various microporous materials studied here are restricted to a function of pore topology and alkane chain length at room temperature. In certain cases, sorption in channels may be a subtle function of experimental conditions, such as different temperatures and sorbate partial pressures. Ferrierite is one possible example of this and certainly merits further investigation.

TABLE 1: Details of Potential Parameters Used in Simulations

internal potential parameters	
bond stretching	
$U_{(\text{stretch})} = \text{constant}$	fixed bond length = 1.53 Å
bond bending	
$U_{(\text{bend})}(\theta_i) = 1/2 k_\theta (\theta_i - \theta_e)^2$	$k_\theta = 62\,500 \text{ K rad}^{-2}$; $\theta_e = 114^\circ$
bond torsion	
$U_{(\text{torsion})}(\phi_i) = a_1(1 + \cos \phi_i) + a_2(1 + \cos 2\phi_i) + a_3(1 + \cos 3\phi_i)$	$a_1 = 355.03 \text{ K}$; $a_2 = -68.19 \text{ K}$; $a_3 = 791.32 \text{ K}$
external potential parameters	
nonbonded interactions	
$U_{(\text{LJ})}(r_{ij}) = 4\epsilon_{ij}[(\sigma_{ij}/r_{ij})^{12} - (\sigma_{ij}/r_{ij})^6]$	$\sigma_{\text{CH}_3} = \sigma_{\text{CH}_2} = 3.93 \text{ Å}$; $\epsilon_{\text{CH}_3} = 114.0 \text{ K}$; $\epsilon_{\text{CH}_2} = 47.0 \text{ K}$; $\sigma_{\text{CH}_3\text{O}} = \sigma_{\text{CH}_2\text{O}} = 3.364 \text{ Å}$; $\epsilon_{\text{CH}_3\text{O}} = \epsilon_{\text{CH}_2\text{O}} = 84.0 \text{ K}$

While a complete description of the interactions in host-guest systems necessitates dynamic information, such as that obtained from diffusion studies, these static simulations using the CB-MC method provide a very useful insight into the behavior of the sorbed species.

Appendix: Zeolite Models and Potential Parameters

The all-silica models of the various zeolites were normally taken from the crystallographic information in the Solids Builder Module of the BIOSYM Catalysis and Sorption Project software.¹⁷ This database of zeolite structures generally contains the crystallographic data for the as-synthesized aluminosilicate structure: for our calculations we used MOR,¹⁸ RHO,¹⁹ LTA,²⁰ and FER.²¹ In all these cases, all aluminum atoms are replaced with silicon. For faujasite we use the purely siliceous structure determined by Cheetham *et al.*²² on the basis of a neutron diffraction and MAS-NMR study. The dimensions of the various model simulation boxes are given in Table I of ref. 6.

The intermolecular potential parameters are given in Table 1. The alkane chains are comprised of united $\text{CH}_{2/3}$ atoms. The nonbonded Lennard-Jones interactions were truncated at 13.8 Å, and the usual tail corrections were applied to account for interactions beyond this cutoff distance. The potential parameters shown in Table 1 were optimized to reproduce the heats of adsorption of *n*-alkanes in silicalite.⁵

References and Notes

- (1) Titiloye, J. O.; Parker, S. C.; Stone, F. S.; Catlow, C. R. A. *J. Phys. Chem.* **1991**, *95*, 4038–4044.
- (2) June, R. L.; Bell, A. T.; Theodorou, D. N. *J. Phys. Chem.* **1992**, *96*, 1051–1060.
- (3) Nicholas, J. B.; Trouw, F. R.; Mertz, J. E.; Iton, L. E.; Hopfinger, A. J. *J. Phys. Chem.* **1993**, *97*, 4149–4163.
- (4) Hernandez, E.; Catlow C. R. A. *Proc. R. Soc. London. Ser. A* **1995**, *448*, 143–160.
- (5) Smit, B.; Siepmann, J. I. *J. Phys. Chem.* **1994**, *98*, 8442–8452.
- (6) Bates, S. P.; van Well, W. J. M.; van Santen, R. A.; Smit, B. *J. Am. Chem. Soc.* **1996**, *118*, 6753–6759.
- (7) Smit, B. *Mol. Phys.* **1995**, *85* (1), 153–172.
- (8) Bezus, A. G.; Kiselev, A. V.; Lopatkin, A. A.; Du, P. Q. *J. Chem. Soc., Faraday Trans. 2* **1978**, *74*, 367–379.
- (9) Eder, F.; Stockenhuber, M.; Lercher, J. A. In *Zeolites: A Refined Tool for Designing Catalytic Sites*; Studies in Surface Science & Catalysis; Bonneviot, L., Kaliaguine, S., Eds.; Elsevier: Amsterdam, 1995; pp 495–500.
- (10) Compton, D. A. C.; Montero, S.; Murphy, W. F. *J. Phys. Chem.* **1980**, *84*, 3587.
- (11) Bartell, L. S.; Kohl, D. A. *J. Chem. Phys.* **1958**, *35*, 3097.
- (12) Mooiweer, H. H.; de Jong, K. P.; Kraushaar-Czarnetzki B.; Stork, W. H. J.; Krutzen, B. C. H. In *Zeolites and Related Microporous Materials: State of The Art 1994*; Studies in Surface Science & Catalysis; Weitkamp, J., Karge, H. G., Pfeifer H., Hölderich, W., Eds.; Elsevier: Amsterdam, 1994; pp 2327–2334.

(13) Demontis, P.; Suffritti, G. B. In *Zeolites and Related Microporous Materials: State of The Art 1994*; Studies in Surface Science & Catalysis; Weitkamp, J., Karge, H. G., Pfeifer H., Hölderich, W., Eds.; Elsevier: Amsterdam, 1994; pp 2107–2113.

(14) Abrams L.; Corbin, D. R. *J. Catal.* **1991**, *127*, 9–21.

(15) Maginn, E. J.; Bell, A. T.; Theodorou, D. N. In *Zeolites and Related Microporous Materials: State of The Art 1994*; Studies in Surface Science & Catalysis; Weitkamp, J., Karge, H. G., Pfeifer, H., Hölderich, W., Eds.; Elsevier: Amsterdam, 1994; pp 2099–2105.

(16) Maginn, E. J.; Bell, A. T.; Theodorou, D. N. *J. Phys. Chem.* **1995**, *99*, 2057–2079.

(17) Biosym Technologies/Molecular Simulations Inc.; 9865 Scranton Road, San Diego, CA.

(18) Alberti, A.; Davoli, P.; Vezzalini, G. *Z. Kristallogr.* **1986**, *175*, 249–256.

(19) McCusker, L. B.; Baerlocher, C. *New Developments in Zeolite Science and Technology*, Proceedings of the 6th International Zeolite Conference; Olsen, D., Bisio, A., Eds.; Butterworth: Guildford, U.K., 1984; pp 812–822.

(20) Gramlich, V.; Meier, W. M. *Z. Kristallogr., Kristallgeometrie, Kristallphys., Kristallchem.* **1971**, *133*, 134–149.

(21) Vaughan, P. A. *Acta Crystallogr.* **1966**, *21*, 983–990.

(22) Hriljac, J. A.; Eddy, M. M.; Cheetham, A. K.; Donohue, J. A.; Ray, G. J. *J. Solid State Chem.* **1993**, *106*, 66–72.

JP961386W